PCCP

Accepted Manuscript

ROYAL SOCIETY OF CHEMISTRY

www.rsc.org/pccp

Cloud condensation nucleation activities of calcium carbonate and its atmospheric ageing products

M. J. Tang[1], J. Whitehead[2], N. M. Davidson[3], F. D. Pope[3], M. R. Alfarra[2,4], G. McFiggans[2], M. Kalberer[1]

1 Department of Chemistry, University of Cambridge, Cambridge CB2 1EW, UK

2 School of Earth, Atmospheric and Environmental Sciences, University of Manchester, Manchester M13 9PL, UK

3 School of Geography, Earth and Environmental Sciences, University of Birmingham, Birmingham B15 2TT, UK

4 National Centre for Atmospheric Science, University of Manchester, Manchester M13 9PL, UK

Correspondence to: M. Kalberer (Markus.Kalberer@atm.ch.cam.ac.uk)

Abstract

Aerosol particles can serve as cloud condensation nuclei (CCN) to form cloud droplets, and its composition is a main factor governing whether an aerosol particle is an effective CCN. Pure mineral dust particles are poor CCN; however, changes in chemical composition of mineral dust aerosol particles, due to heterogeneous reactions with reactive trace gases in the troposphere, can modify their CCN properties. In this study we investigated the CCN activities of $CaCO_3$ (as a surrogate for mineral dust) and its six atmospheric ageing products: $Ca(NO_3)_2$, $CaCl_2$, $CaSO_4$, $Ca(CH_3SO_3)_2$, $Ca(HCOO)_2$, and $Ca(CH_3COO)_2$. $CaCO_3$ has a very low CCN activity with a hygroscopicity parameter (κ)

of 0.001-0.003. The CCN activities of its potential atmospheric ageing products are significantly higher. For example, we determined that $Ca(NO_3)_2$, $CaCl_2$ and $Ca(HCOO)_2$ have κ values of ~0.50, similar to that of $(NH_4)_2SO_4$. $Ca(CH_3COO)_2$ has slightly lower CCN activity with a κ value of ~0.40, and the κ value of $CaSO_4$ is around 0.02. We further show that exposure of $CaCO_3$ particles to N_2O_5 at 0% relative humidity (RH) significantly enhances their CCN activity, with κ values increasing to around 0.02-0.04. Within the experimental uncertainties, it appears that the variation in exposure to N_2O_5 from ~550 to 15000 ppbv·s does not change the CCN activities of aged $CaCO_3$ particles. This observation indicates that the $CaCO_3$ surface may be already saturated at the shortest exposure. We also discussed the atmospheric implications of our study, and suggested that the rate of change in CCN activities of mineral dust particles in the troposphere is important to determine their roles in cloud formation.

1 Introduction

Atmospheric aerosol particles impact the energy balance of the earth by scattering and absorbing solar and terrestrial radiation (direct radiative effect) and by affecting cloud microphysics, albedo, and lifetime (indirect radiative effect).[1] The indirect radiative effect arises from the ability of aerosol particles to serve as cloud condensation nuclei (CCN) to form liquid clouds and ice nuclei (IN) to form ice clouds.[2] The indirect radiative forcing of aerosol particles has the largest uncertainty in current estimates of radiative forcing, and this lack of knowledge is one of the bottlenecks for reliable and accurate projections of climate change.[1] The interaction of aerosol particles with clouds further impacts precipitation and the hydrological cycle.[3] The ability of an aerosol particle to be activated and thus become a cloud droplet under certain supersaturation depends primarily on its size

but also on its hygroscopicity.[4, 5] A detailed knowledge of how CCN activity varies with the compositions and mixing state of aerosol particles is therefore required to fully understand their roles in liquid cloud formation.

On a mass basis, mineral dust is the most abundant type of aerosol particles in the troposphere, with a flux of ~2000 Tg yr^{-1}.[6] Dust particles are mainly emitted from arid and semi-arid regions and have an average lifetime of 2-7 days.[7] They can be transported over thousands of kilometres and therefore have global impacts.[8, 9] For example, mineral dust aerosols can impact the climate directly by absorbing and scattering solar and terrestrial radiation [10, 11] and indirectly by serving as CCN.[12-15] The deposition of dust particles during transport is a major source of nutrients (e.g., Fe and P) for many open-oceanic regions, significantly impacting oceanic biogeochemical cycles and their feedbacks on climate.[16]

Mineral dust particles undergo heterogeneous reactions with reactive trace gases during transport.[17, 18] These reactions can influence the concentrations of several important trace gases in the troposphere,[19, 20] and modify the chemical compositions of dust particles,[21-23] leading to changes of their hygroscopicity and CCN activities,[24-26] ice nucleation ability,[27-29] and solubility and bio-availability of nutrients.[30]

Calcium carbonate ($CaCO_3$), an important component in mineral dust particles,[31, 32] has a very low hygroscopicity.[33, 34] The tropospheric loading of $CaCO_3$ is estimated to be 1.3 Tg, which is ~8% of the total loading of mineral dust particles.[35] In this study we have investigated the CCN activity of $CaCO_3$ and its aging products, because atmospheric heterogeneous chemistry of $CaCO_3$ has been widely studied [18] but it is not very clear how these heterogeneous reactions will change its CCN activity. It is suggested that the formation of more soluble species, due to heterogeneous reactions with acidic trace gases

during atmospheric transport, would enhance the CCN activity of mineral dust particles.[36, 37] This is supported by experimental work. For example, it is found that the CCN activity of $Ca(NO_3)_2$ and $CaCl_2$ is similar to that of $(NH_4)_2SO_4$.[33] In this work we determine the CCN activity of $CaCO_3$ and six of its atmospheric ageing products: (i) $Ca(NO_3)_2$, formed in the reactions of $CaCO_3$ with HNO_3,[38-40] N_2O_5,[41, 42] and NO_2;[43, 44] (ii) $CaCl_2$, formed in the reaction of $CaCO_3$ with HCl;[45, 46] (iii) $CaSO_4$, formed in the heterogeneous oxidation of SO_2 on $CaCO_3$ surface by O_3;[47, 48] and (iv-vi) $Ca(CH_3SO_3)_2$, $Ca(HCOO)_2$, and $Ca(CH_3COO)_2$, formed in the reactions of $CaCO_3$ with methanesulfonic acid,[49] HCOOH,[50] and CH_3COOH.[38, 51] Abundant organic compounds were found to be associated with ambient mineral dust particles.[52] The CCN activities of $Ca(NO_3)_2$, $CaCl_2$, and $CaSO_4$ have only been reported by one previous study,[33] and more independent investigation is warranted. The CCN activities of $Ca(CH_3SO_3)_2$, $Ca(HCOO)_2$, and $Ca(CH_3COO)_2$ have not been investigated so far, although the hygroscopicity of $Ca(CH_3SO_3)_2$ under subsaturation conditions has been studied.[53]

In addition, for the first time, we investigate the CCN activity change of $CaCO_3$ aerosol particles after exposure to N_2O_5. N_2O_5 is an important nocturnal reservoir of nitrogen oxides in the troposphere.[54, 55] Due to its significance in the troposphere, kinetics and mechanisms of the heterogeneous reaction of N_2O_5 with mineral dust have been extensively studied. It is widely recognised that this reaction leads to the formation of nitrate on mineral dust particles,[42, 56, 57] in addition to efficient removal of reactive nitrogen species from the gas phase.[41, 58-61] However, it has not been explored yet whether (and how fast) this reaction will change the CCN activity of mineral dust particles. We show in this study that heterogeneous reaction with N_2O_5 can enhance the CCN activity of mineral dust

particles, although the measured increase is likely too small to significantly impact $CaCO_3$ particle activation in the atmosphere.

2 Experimental section

2.1 Cloud condensation nucleation measurement

Aerosol particles, except $CaCO_3$ (the generation of which is described in Section 2.2), were generated by atomizing aqueous solutions of the pure species of interest in water (with concentrations of 10-20 mg per litre), using a commercial atomizer (TSI 3076). The aerosol flow (3000 cm^3/min) exiting the atomizer was transported through two diffusion dryers and then split. One flow passed through a filter, across a temperature and relative humidity (RH) sensor, and then into the exhaust. The measured RH was always below 5%. The other flow (800 cm^3/min) was delivered through a Kr-85 aerosol neutralizer and then a differential mobility analyser (DMA, TSI 3081) to produce monodisperse aerosol particles. The sheath flow of the DMA was set to 8 L/min.

After exiting the DMA, the aerosol flow was split using a brass Y-piece. A flow of 300 cm^3/min was sampled into a condensation particle counter (CPC, TSI 3775) to measure the total particle (i.e., condensation nuclei, CN) number concentration, and the other flow (500 cm^3/min) was sampled into a cloud condensation nuclei counter (CCNc) to measure the cloud condensation nuclei (CCN) number concentration. The particle size range for this CPC is stated by the manufacturer to be from 4 nm to >3000 nm. The design of the CCNc (Droplet Measurement Technologies, model 100) is based on the instrument developed by Roberts and Nenes.[62] In brief, the CCNc creates a constant supersaturation to which aerosol particles are exposed. Aerosol particles could then be activated to cloud droplets, the concentration of which is detected by an optical particle counter. The supersaturation (SS)

which this instrument can create could be adjusted between 0.07% and 2% with increments of a stated resolution of 0.01%. Details of the instrument are provided elsewhere.[63] In this study a typical activation curve contains measurements at 12-15 different SS.

2.1.1 CCNc calibration

The CCNc was calibrated using the method described in detail elsewhere.[63] In brief, measured critical supersaturations (SSc) of monodisperse $(NH_4)_2SO_4$ particles with dry particle mobility diameters (d_m) of 40, 50, 60, 70 and 75 nm were compared with theoretical SSc values at 298 K, as predicted by the ADDEM model.[64] It was found that the measured SSc were always 0.02% (on an absolute scale) higher than theoretical values for SSc ranging from ~0.2% to >0.6%. Therefore, all the experimentally determined SSc values have been subtracted by 0.02% to give corrected SSc values, which are reported here.

2.2 Aerosol flow tube

In this section we describe the set-up used to determine the CCN activity of fresh and aged $CaCO_3$ particles due to the reaction with N_2O_5. All other minerals were produced as described in 2.1 and did not pass through the flow tube.

2.2.1 $CaCO_3$ aerosol generation

The dust disperser used to produce $CaCO_3$ aerosol particles is similar to those described in previous studies.[41, 42] As shown in Figure 1, dry $CaCO_3$ powder was placed in a 500 mL Erlenmeyer flask and stirred using a magnetic stirrer. A N_2 flow (F1) of 1500 cm^3/min was delivered through a 1/8'' stainless steel tube into the flask to entrain dust particles into the air. The tip of this tube was connected to a home-made nozzle with a diameter of ~0.3 mm to increase the linear flow velocity. The resulting aerosol flow was delivered through a glass vessel with a volume of ~3 L (length: 40 cm; inner diameter: 10 cm), serving to

smooth spikes in the dust aerosol concentrations. The flow exiting the glass vessel could be passed through a filter to remove all the particles, or alternatively the filter could be bypassed. The aerosol flow was then transported through a cyclone (TSI 1031097) to remove large particles. After that, the flow was passed through a Kr-85 neutralizer into a differential mobility analyser (DMA, TSI 3081) to generate monodisperse dust particles. Depending on the sheath flow, particles in the range approximately from 10 to 1000 nanometers in mobility diameter can be selected by this DMA. The sheath flow of the DMA was set to 15 L/min.

2.2.2 Aerosol flow tube

The dust aerosol flow exiting the DMA was delivered into an aerosol flow tube via a side arm, as shown in Figure 1. The aerosol flow tube was described previously.[57, 65] In brief, the flow tube, with an inner diameter of 3.0 cm and a length of 100 cm, was mounted horizontally. The total flow in the flow tube was 1500 cm^3/min, giving a linear flow velocity of 3.54 cm s^{-1}. The Reynolds number was 76, suggesting that the flow was laminar. The entrance length, required to fully develop the laminar flow, was ~13 cm, and the mixing length was ~16 cm. Only the middle part of the flow tube (20-70 cm) was used to vary the interaction time of $CaCO_3$ particles with N_2O_5.

A small N_2 flow (F2, typically 5-10 cm^3/min) was used to elute gaseous N_2O_5 from the crystalline N_2O_5 sample kept at -50 ^oC in a cryostat. The N_2O_5 flow was delivered into the centre of the flow tube through a 1/8'' Teflon tube in a stainless steel sliding injector. The injector position could be adjusted to vary the interaction time between airborne $CaCO_3$ particles and N_2O_5. At the end of the flow tube, one flow (~500 cm^3/min) was sampled into a heated reactor (100 ^oC), mixed with NO in excess, and then sampled into a NOx analyser

(Model 200E, Teledyne Instruments, USA). N_2O_5 concentrations were determined by the change of NO concentrations, as shown by reactions (R1) and (R2), where M is the third collisional body. Synthesis and purification of N_2O_5 crystals and detection of gaseous N_2O_5 are described in our previous work.[57, 65] The wall loss rate was determined to be around 0.01 s^{-1} at 0% RH, by measuring N_2O_5 concentrations at different injection positions.

$N_2O_5 + M \rightarrow NO_2 + NO_3 + M$ (R1)

$NO + NO_3 \rightarrow NO_2 + NO_2$ (R2)

Another flow (~800 cm^3/min) was used to measure the CCN activity of fresh and aged $CaCO_3$ particles, and the remaining flow (~200 cm^3/min) went into the exhaust through the end of the flow tube. The 800 cm^3/min flow was first delivered through two tandem glass tubes (denuders), the inner walls of which were sandblasted and coated with Na_2CO_3 to remove N_2O_5 in the gas flow. Removal of N_2O_5 to terminate the heterogeneous reaction is critical for the CCN measurement, because inside the CCNc column heterogeneous hydrolysis of N_2O_5 can be very fast, leading to the formation of additional nitrate on the particles and thus causing measurement artifacts. Denuders used in this study have a length of 70 cm and an inner diameter of 9 mm. Theoretical estimations [66] suggests that only 0.6% N_2O_5 is left after the flow exits one denuder. The denuder capacity was experimentally determined. It is confirmed that 500 ppbv N_2O_5 could be completely removed for at least six hours continuously (i.e. below 0.5 ppbv, which is detection limit of the NOx analyser). Denuders were replaced with fresh ones every day before starting the experiments.

2.3 Data analysis and *κ*-Köhler theory

CCN activation curves of monodisperse aerosol particles were generated by measuring the ratio of activated particle number concentration (CCN) to the total particle number

concentration (CN) with a time resolution of 1 s at different SS. Measurements lasted for 5-10 minutes for each SS. Only the [CCN]/[CN] data in the last minute for each SS were used to generate an average activation fraction (i.e. [CCN]/[CN]), to ensure that the SS were stable.

Aerosol particles generated by the atomizer have very stable concentrations over time, and typical number concentrations of monodisperse particles used in this study were 1000-3000 cm^{-3}. It is nontrivial to generate $CaCO_3$ dust particles with stable concentrations using dry dispersion.[42, 60] In this study, when the supersaturation in the CCNc column became stable (usually 2-3 min after the supersaturation was set), $CaCO_3$ powder in the flask was stirred for ~30 s to generate dust aerosols. The number concentration of $CaCO_3$ particles increased promptly and then decayed exponentially. An example dataset of [CCN], [CN] and [CCN]/[CN] for $CaCO_3$ particles as a function of time is given in Section 3.3.

A Boltzmann sigmoid curve of the following form was then used to fit the activation fraction against SS:[33]

$$y = A2 + \frac{A1 - A2}{1 + \exp[(x - x0)/dx]} \qquad \text{(E1)}$$

where y is the activation fraction ([CCN]/[CN]), x is the supersaturation (SS). $A1$, $A2$, dx, and $x0$ are constants which are determined by the fitting, and $x0$ is equal to the critical supersaturation, SSc.

2.3.1 κ-Köhler theory

The CCN activity of a particle can be described by the single hygroscopicity parameter, κ, which is defined through the water activity of the particle, a_w:[67]

$$\frac{1}{a_w} = 1 + \kappa \frac{V_s}{V_w} \qquad \text{(E2)}$$

where V_s and V_w are the volume of the dry particle and that of water contained by the particle. The saturation ratio over a curved surface, is given by

$$S(D) = a_w exp\left(\frac{4\sigma M_w}{RT\rho_w D}\right) \qquad \text{(E3)}$$

where $S(D)$ is the saturation ratio over a particle with a diameter of D, σ is the surface tension of the particle, M_w is the molecular weight of water, ρ_w is the water density, R is the gas constant, and T is temperature. Combination of Eqs. (2-3) describes $S(D)$ as a function of κ, the droplet diameter, D, and the dry particle diameter, D_{dry}:[67]

$$S(D) = \frac{D^3 - D_{dry}^3}{D^3 - D_{dry}^3 \cdot (1-\kappa)} \cdot exp\left(\frac{A}{D}\right) \qquad \text{(E4)}$$

where A is a constant equal to 2.1 nm at 298.15 K, assuming that the surface tension of the particle is equal to that of pure water at 298.15 K, i.e. 0.072 J m^{-2}.[33] This framework, introduced by Petters and Kreidenweis (2007), is usually called κ-Köhler theory. The Frenkel-Hasley-Hill (FHH) adsorption activation theory has been suggested as an alternative (and arguably more suitable) framework to describe the CCN activity of dust particles.[68, 69] However, a recent study suggests that the κ-Köhler theory is a suitable framework to describe the CCN activity not only of water-soluble particles but also of dust particles.[70] It is beyond the scope of our current work to discuss whether the κ-Köhler theory or the FHH adsorption theory is a more suitable framework to describe the CCN activity of mineral dust particles. The κ-Köhler theory only requires one parameter to describe the CCN activity while the FHH adsorption activation theory needs two. Therefore, in our work the single hygroscopicity parameter (κ) is used to represent the CCN activity of fresh and aged $CaCO_3$ particle. The values of κ can vary from 0 to ~1.4, increasing with the CCN activity of the particle. For example, $(NH_4)_2SO_4$ and $Ca(NO_3)_2$ have κ values of ~0.5,[67] while $CaCO_3$ has a very low κ value of ~0.001.[33]

A given pair of D_{dry} and κ is inserted into Eq. (E4), and D is increased from D_{dry} to find the maximum point of the $S(D)$ curve, S_{max}. The critical supersaturation ratio, SSc, is equal to S_{max}-1. In this study, a range of D_{dry} (from 20 to 439 nm with an increment of 1 nm) and κ (from 0 to 1.99 with an increment of 0.01 and from 0 to 0.0499 with an increment of 0.0001) were inserted into Eq. (E4) using the same procedure to generate a lookup table of SSc as a function of D_{dry} and κ.[64] This table was then used to derive the κ value from D_{dry} (assumed to be the mobility diameter of dry particles) and SSc which was experimentally determined.

2.4 Chemicals

Ammonium sulfate(>99.0%), calcium nitrate hydrate (>99.997%), calcium chloride dehydrate (>99%), calcium sulfate dihydrate (>99%), calcium acetate monohydrate (>99%) and calcium formate (>99.0%) were purchased from Sigma-Aldrich UK. Calcium methanesulfonate (>98%) was purchased from Tokyo Chemical Industry UK Ltd. $CaCO_3$ (precipitated calcium carbonate, >99.0%) particles were offered by Omya UK Limited. To check the purity of $CaCO_3$, $CaCO_3$ powder was extracted in Milli-Q water (continuously stirred) for 90 min, and the solution was analysed by ion chromatography (IC). The impurity level was 0.08±0.02, 0.25±0.09, 0.55±0.40, 0.59±0.21 and 2.92±1.87 μg per gram $CaCO_3$ for Na^+, K^+, Cl^-, NO_3^- and SO_4^{2-}, respectively. The amounts of NH_4^+ and PO_4^{3-} were both below the detection limit. All the chemicals were used as received, and HPLC grade water (Fisher Scientific) was used to prepare solutions.

3 Results and Discussion

3.1 CCN activity of $Ca(NO_3)_2$, $CaCl_2$, and $CaSO_4$

Typical activation curves of 50 nm $CaCl_2$ (blue triangles) and 200 nm $CaSO_4$ (black squares) are displayed in Figure 2. Dry particle diameters were selected in such a way that

the measured SSc roughly falled into 0.3-0.6 %. The activation curve for 50 nm $CaCl_2$ particles shows a small plateau for SS between 0.30% and 0.45%. Similar phenomena were also observed for other types of aerosol particles. This is due to the presence of double-charged particles which have the same electrical mobility as single-charged particles. Double-charged particles have larger diameters and are activated at lower supersaturation. The effect of double charge can be corrected, and we find that the difference in derived SSc with and without double charge correction is <0.02% and thus negligible for all types of aerosol particles generated using the atomizer. This is because the fraction of multi-charged particles is small. Similar observations were also reported by Sullivan et al.[71]

All the mobility diameters, SSc, and the corresponding hygroscopicity parameter (κ) are summarized in Table 1. In this work particle sizes always refer to mobility diameters of dry particles. The κ values of $Ca(NO_3)_2$, $CaCl_2$, and $CaSO_4$ reported by Sullivan et al.[33, 72] are also included in Table 1 for comparison. Our determined κ is 0.57-0.59 for $Ca(NO_3)_2$ and 0.51-0.54 for $CaCl_2$, in good agreement with 0.44-0.64 for $Ca(NO_3)_2$ and 0.46-0.58 for $CaCl_2$ reported by Sullivan et al.,[33] although mobility diameters used in our study are 50-70 nm while they used 75-154 nm.[33] Both $Ca(NO_3)_2$ and $CaCl_2$ are very CCN active and have similar hygroscopicity to $(NH_4)_2SO_4$,[67] a common component in tropospheric aerosol particles.

The hygroscopicity parameter of $CaSO_4$ was determined at three different particle diameters (100, 150 and 200 nm), with values of 0.012-0.034. Sullivan et al.[72] used a similar method to generate $CaSO_4$ particles and their reported κ, 0.0045±0.0012, is lower than that determined by our study. However, as mentioned above, their reported CCN

activities of $CaCl_2$ and $Ca(NO_3)_2$ in another study [33] agree well with our work. It is not clear why the CCN activity of $CaSO_4$ measured by Sullivan et al.[72] is different from this work. $CaSO_4$ is known to be very insoluble, but hygroscopic once deliquesced. It is likely that kinetics will play an important role in its activation. Further measurements may help resolve this discrepancy.

3.2 CCN activity of $Ca(CH_3SO_3)_2$, $Ca(HCOO)_2$, and $Ca(CH_3COO)_2$

Figure 2 also displays an activation curve of 70 nm $Ca(CH_3SO_3)_2$ particles (red circles). The measured hygroscopicity, represented by κ, is 0.30-0.38 for $Ca(CH_3SO_3)_2$ (Table 1), which is significantly lower than those for $Ca(NO_3)_2$ and $CaCl_2$ but much higher than that for $CaSO_4$. To our knowledge, the hygroscopicity of $Ca(CH_3SO_3)_2$ has never been investigated previously under supersaturation conditions.

We have also measured the hygroscopicity of $Ca(HCOO)_2$ and $Ca(CH_3COO)_2$, the CCN activities of which have not been studied previously. A typical activation curve for 50 nm $Ca(CH_3COO)_2$ particles (orange diamonds) is displayed in Figure 2. The determined SSc, corresponding diameters, and κ are summarized in Table 1. The hygroscopicity of $Ca(HCOO)_2$ is determined to be 0.47-0.52, similar to those for $(NH_4)_2SO_4$, $Ca(NO_3)_2$ and $CaCl_2$, and the hygroscopicity for $Ca(CH_3COO)_2$ is slightly lower, with κ values of 0.34-0.37.

3.3 CCN activity of fresh and aged $CaCO_3$

3.3.1 CCN activity of fresh $CaCO_3$

Figure 3 shows the measured [CN], [CCN], and [CCN]/[CN] of 200 nm fresh $CaCO_3$ particles as a function of time at a SS of 0.50%. Although the particle number concentration, i.e. [CN], decreased from ~1600 to ~1100 cm^{-3} in 1 min, the activation fraction,

[CCN]/[CN] was very stable, with an average value of 0.321±0.016. Similar data were collected at 12-15 different supersaturations to generate an activation curve, and a typical activation curve for 200 nm fresh $CaCO_3$ particles is shown in Figure 4 (open circles).

A distinctive feature of the activation curve for $CaCO_3$ particles is that the effect of multicharged particles (as indicated by the plateau for SS between 0.50-0.65 %) is more significant than those for other types of aerosol particles generated using an atomizer. Similar observations were also reported previously.[71] The derived SSc after removing the contribution of multicharged particles is <0.02% larger than those without any correction. The difference is negligible compared to the variation in SSc for 200 nm $CaCO_3$ particles measured in different experiments.

As summarized in Table 2, the κ values for $CaCO_3$ particles are in the range of 0.0013-0.0033. Sullivan et al.[33] measured the CCN activity of $CaCO_3$ aerosol particles generated using a similar method, and κ values of 0.0008-0.0018 were reported. $CaCO_3$ samples used by Sullivan et al.[33] were synthesized using a similar method but provided by a different company. However, κ values determined by the two studies agree reasonably well. Water-soluble impurities of $CaCO_3$ particles used in our study have been quantified, as discussed in Section 2.4. In addition, Zhao et al.[34] developed a novel method to generate pure $CaCO_3$ aerosol particles, and their reported κ values of 0.0019±0.0007 are also in good agreement with those measured by our study.

3.3.2 Effect of heterogeneous N_2O_5 uptake on CCN activity of $CaCO_3$

As discussed in the introduction, the uptake of N_2O_5 by mineral dust particles (in this case, $CaCO_3$) leads to the formation of nitrate on particles, probably increasing their CCN activity. This is confirmed by the CCN activation curve (squares in Figure 4) of aged

$CaCO_3$ particles after heterogeneous reaction with N_2O_5 in the aerosol flow tube. Compared to that of fresh $CaCO_3$ particles with the same initial diameter (200 nm), the activation curve of aged $CaCO_3$ particles is substantially shifted to lower SS and thus the SSc has been reduced and the CCN activity has increased due to the reaction with N_2O_5. An interesting feature for the activation curves of fresh and aged $CaCO_3$ particles, as evident from Figure 4, is that the plateau in the fresh $CaCO_3$ curve, caused by the presence of multi-charged particles, has largely disappeared for aged particles. Similar observations were reported in a previous study in which $CaCO_3$ particles were exposed to HNO_3 in an aerosol flow tube,[71] although no explanation was provided. For the same electrical mobility, multi-charged particles have larger diameters than single charged particles. The formation of nitrate on the particles, due to the heterogeneous reactions with N_2O_5 or HNO_3, is proportional to the particle surface area,[18] i.e. proportional to the square of the particle diameter, while the volume (and mass) of the particle is proportional to the cube of the particle diameter. Therefore, the ratio of the mass (and volume) of formed nitrate to that of the initial particle decreases with increasing particle diameter. The κ value of internally mixed particles is determined by the volume fractions of different compositions (and their individual κ values) they contain. After exposure to N_2O_5, $CaCO_3$ particles with larger diameters will have lower nitrate to carbonate volume (and mass) ratios and as a result, lower κ values. The combination of larger diameter (requiring lower SSc to be activated) and lower κ values (requiring higher SSc to be activated) for multicharged aged particles may make them become activated at same/similar supersaturations as single charged aged particles. Consequently, the distinctive plateau which occurred for fresh $CaCO_3$ particles would disappear after the particles were aged.

CCN activities of 200 nm $CaCO_3$ particles, after being exposed to N_2O_5 at 0% RH in the aerosol flow tube, are also summarized in Table 2. N_2O_5 concentrations given in Table 2 refer to initial N_2O_5 concentrations, which are extrapolated to the reaction time of 0 s from the online measured N_2O_5 concentration at each injector position (i.e., reaction time) by taking the wall loss into account. N_2O_5 wall loss in the flow tube has also been taken into consideration when calculating exposures which are also listed in Table 2. Therefore, the exposures are always smaller than the corresponding initial N_2O_5 concentrations multiplied by the reaction time. The amount of N_2O_5 taken up by aerosol particles is negligible compared to the total amount of N_2O_5 introduced into the flow tube because only a few thousand particles per cm^3 were present in the flow tube.

The effect of the heterogeneous reaction with N_2O_5 on the CCN activity of mineral dust particles has not been explored previously. We find that exposure to N_2O_5 increases the CCN activities of $CaCO_3$ particles, with κ increasing from 0.0013-0.0033 to 0.0186-0.0418. Table 2 also reveals that within the experimental uncertainties, κ values remain the same for all $CaCO_3$ particles which reacted with N_2O_5 at 0% RH in the aerosol flow tube, though the N_2O_5 exposure varies from ~550 to ~15000 ppbv·s at 0% RH.

3.3.3 Discussion

A previous study found that exposure to HNO_3 significantly increased the CCN activity of $CaCO_3$ particles, using an aerosol flow tube.[71] At 0% RH, we found that κ only increased to ~0.02-0.04 with exposure to N_2O_5 for up to 15000 ppbv·s, while Sullivan et al.[71] suggested that it increased to ~0.2 with exposure to HNO_3 only for ~300 ppbv·s. This may be explained by the fact that at 0% RH the uptake coefficient on $CaCO_3$ is larger for HNO_3 (0.11) [73] than that for N_2O_5 (0.0048±0.0007) [41].

We show that there is no change in κ within the experimental uncertainties for N_2O_5 exposure varying from ~550 to ~15000 ppbv·s at 0% RH. In contrast, Sullivan et al.[71] suggest that κ increases with exposure (from ~2 to ~300 ppbv·s) for HNO_3 at 0% RH. Wagner et al.[41] suggest that $\gamma(N_2O_5)$ increases from 0.0048±0.0007 at 0% RH to 0.0194±0.0022 at 71% RH for $CaCO_3$ particles. As a result, we expect that the CCN activities of aged $CaCO_3$ particles will increase with RH for the same N_2O_5 exposure. In contrast, Sullivan et al.[71] show that the change in CCN activity of $CaCO_3$ particles due to the reaction with HNO_3 is independent of RH.

Only these two studies have explored how fast heterogeneous reactions change the CCN activities of mineral dust particles, and the apparent differences reported by the two studies highlight the challenges in this type of work. How fast the CCN activity of mineral dust particles change with atmospheric exposure may critically determine the role of mineral dust particles in the formation of cloud droplets, as discussed below.

3.4 Atmospheric implications

Our current work and other previous studies [26, 71] show that the CCN activities of atmospheric aging products of $CaCO_3$ particles, an important component in mineral dust particles, have significantly higher CCN activities than fresh $CaCO_3$ particles. The difference in CCN activity between fresh $CaCO_3$ particles and other Ca-containing compounds listed in Table 1 is mainly due to the difference in solubility.[33, 74] Figure 5 shows SSc as a function of dry particle diameter for different compounds. For a dry particle diameter of 100 nm, the SSc is ~1.59% for fresh $CaCO_3$, 0.77% for $CaSO_4$, 0.65% for aged $CaCO_3$ particles which have been exposed to N_2O_5 at 0% RH, and 0.16% for $Ca(NO_3)_2$, suggesting that heterogeneous reactions could substantially reduce the critical

supersaturation required to activate mineral dust particles to form cloud droplets if heterogeneous aging reactions have completely transformed the $CaCO_3$ particles into more CCN active products. As a result, it might be important for cloud microphysics models to take into account the effect of atmospheric aging processes, if such complete reaction would occur in the atmosphere.

We further demonstrate that not only the scale of the change of CCN activity is important, but also that the rate of the change critically determines its relevance and significance in the atmosphere. In theory, a $CaCO_3$ particle with a κ value of ~0.002 could be converted to a $Ca(NO_3)_2$ particle with a κ value of ~0.5 after sufficient exposure to reactive nitrogen species. However, our N_2O_5 aging experiments show that at 0% RH, exposure to N_2O_5 of 15000 ppbv·s (which corresponds to exposure to a typical tropospheric N_2O_5 concentration of 50 pptv for ~3.5 days, if assuming that a linear extrapolation is valid) only increases the κ value of $CaCO_3$ from ~0.002 to ~0.02. This is far below the κ value for $Ca(NO_3)_2$, which is ~0.5. Most mineral dust aerosol particles in the troposphere are in the supermicron size range and their number concentrations are typically very low. This means that, in practice all dust particles will act as giant CCN even if their κ is effectively zero. Change in κ as small as from 0.002 to 0.02 may not be relevant to the number of activated droplets in any cloud. Thus, the observed moderate increase in κ under dry conditions will likely have no significant effect for an increased activation of mineral dust in the ambient atmosphere. A previous study [41] suggests that $\gamma(N_2O_5)$ on $CaCO_3$ particles increases with RH, and thus we expect that the effect of reaction with N_2O_5 on the CCN activity will increase at higher RH. Thus, the CCN activity of a dust particle in the troposphere depends on its exposure history to acidic gases and, critically, how fast the exposure changes its CCN activity. Figure 6

shows a schematic diagram of three theoretical representative types of CCN activity change for dust particles. We would like to emphasise that Figure 6 is only for illustrative purposes and is not constructed from experimental data.

If the change in CCN activity is very fast (Type II, Figure 6), then only the initial and final CCN activities need to be considered for atmospheric modelling. For example, Sullivan et al.[71] suggest that $CaCO_3$ particles will be converted to a hygroscopic particle (κ >0.1) after being exposed to 10 pptv HNO_3 for 4 h or 1 ppbv HNO_3 for 3 min. For such efficient chemical reactions, most (if not all) of particles in the troposphere can be treated as particles with a κ value of >0.1.

In contrast, if the change is insignificant during atmospherically relevant exposures (Type III, Figure 6), then the effect of this reaction does not need to be taken into account. For example, although the heterogeneous reaction of NO_3 radicals with mineral dust may lead to the formation of nitrate on the particles, the concentration of NO_3 radicals is much lower than that of N_2O_5 [54] and the uptake coefficient for NO_3 is similar to that for N_2O_5.[75] Therefore, the CCN activity change of dust particles due to the reaction with NO_3 radicals in the troposphere may be negligible, compared to that due to the reaction with N_2O_5.

If the change is substantial and varies significantly with exposure in the atmosphere (Type II, Figure 6), then the rate of change, which depends on concentrations of acidic gases, RH, and kinetics of relevant heterogeneous reactions, should be taken into consideration in atmospheric models.

Atmospheric dust particles consist of a variety of minerals.[31, 32] The CCN activities vary with minerals,[68, 70, 76] and the heterogeneous reactivities with acidic gases, for example, HNO_3 [18] and N_2O_5,[61] also change with different minerals. Previous [24, 33, 43] and our work

focuses on $CaCO_3$, probably the most reactive mineral (but not the most abundant one) in dust particles. More abundant minerals, e.g., illite, kaolinite, and SiO_2,[35] deserve further investigation.

4 Conclusion

In this work we investigated the CCN activities of $CaCO_3$ particles and six calcium-containing salts, including $Ca(NO_3)_2$, $CaCl_2$, $CaSO_4$, $Ca(CH_3SO_3)_2$, $Ca(HCOO)_2$ and $Ca(CH_3COO)_2$, which are possible atmospheric aging products of $CaCO_3$. While the CCN activity of $CaCO_3$ is very low, with a κ value of ~0.002, the CCN activities of these products are all higher than that of fresh $CaCO_3$ particles and vary over a wide range.

We have further explored the CCN activity change of $CaCO_3$ as a result of reaction with N_2O_5. Exposure of $CaCO_3$ particles to N_2O_5 at 0% RH increases their CCN activities, with κ increasing from ~0.002 to ~0.03. At 0% RH the CCN activities of aged $CaCO_3$ particles do not vary significantly with exposure, indicating that at 0% RH the heterogeneous reaction of $CaCO_3$ with N_2O_5 may be limited to the particle surface. Our study suggests that the CCN activities of mineral dust particles can be only slightly enhanced during a realistic atmospheric lifetime due to heterogeneous reactions with acidic trace gases such as N_2O_5.

Acknowledgement

Financial support provided by the Isaac Newton Trust (Trinity College, University of Cambridge, UK) and the European Research Council (ERC starting grant 279405) is acknowledged.

Reference

1. IPCC, *Climate Change 2013: The Physical Science Basis*, Cambridge University Press, Cambridge, UK, 2013.
2. U. Lohmann and J. Feichter, *Atmos. Chem. Phys.*, 2005, **5**, 715-737.
3. D. Rosenfeld, U. Lohmann, G. B. Raga, C. D. O'Dowd, M. Kulmala, S. Fuzzi, A. Reissell and M. O. Andreae, *Science*, 2008, **321**, 1309-1313.
4. U. Dusek, G. P. Frank, L. Hildebrandt, J. Curtius, J. Schneider, S. Walter, D. Chand, F. Drewnick, S. Hings, D. Jung, S. Borrmann and M. O. Andreae, *Science*, 2006, **312**, 1375-1378.
5. G. McFiggans, P. Artaxo, U. Baltensperger, H. Coe, M. C. Facchini, G. Feingold, S. Fuzzi, M. Gysel, A. Laaksonen, U. Lohmann, T. F. Mentel, D. M. Murphy, C. D. O'Dowd, J. R. Snider and E. Weingartner, *Atmos. Chem. Phys.*, 2006, **6**, 2593-2649.
6. C. Textor, M. Schulz, S. Guibert, S. Kinne, Y. Balkanski, S. Bauer, T. Berntsen, T. Berglen, O. Boucher, M. Chin, F. Dentener, T. Diehl, R. Easter, H. Feichter, D. Fillmore, S. Ghan, P. Ginoux, S. Gong, A. Grini, J. Hendricks, L. Horowitz, P. Huang, I. Isaksen, I. Iversen, S. Kloster, D. Koch, A. Kirkevåg, J. E. Kristjansson, M. Krol, A. Lauer, J. F. Lamarque, X. Liu, V. Montanaro, G. Myhre, J. Penner, G. Pitari, S. Reddy, Ø. Seland, P. Stier, T. Takemura and X. Tie, *Atmos. Chem. Phys.*, 2006, **6**, 1777-1813.
7. N. Huneeus, M. Schulz, Y. Balkanski, J. Griesfeller, J. Prospero, S. Kinne, S. Bauer, O. Boucher, M. Chin, F. Dentener, T. Diehl, R. Easter, D. Fillmore, S. Ghan, P. Ginoux, A. Grini, L. Horowitz, D. Koch, M. C. Krol, W. Landing, X. Liu, N. Mahowald, R. Miller, J. J. Morcrette, G. Myhre, J. Penner, J. Perlwitz, P. Stier, T. Takemura and C. S. Zender, *Atmos. Chem. Phys.*, 2011, **11**, 7781-7816.
8. I. Uno, K. Eguchi, K. Yumimoto, T. Takemura, A. Shimizu, M. Uematsu, Z. Liu, Z. Wang, Y. Hara and N. Sugimoto, *Nature Geosci.*, 2009, **2**, 557-560.
9. J. M. Prospero and P. J. Lamb, *Science*, 2003, **302**, 1024-1027.
10. Y. Balkanski, M. Schulz, T. Claquin and S. Guibert, *Atmos. Chem. Phys.*, 2007, **7**, 81-95.
11. I. N. Sokolik and O. B. Toon, *Nature*, 1996, **381**, 681-683.
12. K. A. Koehler, S. M. Kreidenweis, P. J. DeMott, M. D. Petters, A. J. Prenni and C. M. Carrico, *Geophys. Res. Lett.*, 2009, **36**, L08805, doi: 08810.01029/02009gl037348.
13. C. H. Twohy, S. M. Kreidenweis, T. Eidhammer, E. V. Browell, A. J. Heymsfield, A. R. Bansemer, B. E. Anderson, G. Chen, S. Ismail, P. J. DeMott and S. C. Van den Heever, *Geophys. Res. Lett.*, 2009, **36**, L01807, doi: 01810.01029/02008gl035846.
14. D. J. Cziczo, K. D. Froyd, C. Hoose, E. J. Jensen, M. Diao, M. A. Zondlo, J. B. Smith, C. H. Twohy and D. M. Murphy, *Science*, 2013, **340**, 1320-1324.
15. J. M. Creamean, K. J. Suski, D. Rosenfeld, A. Cazorla, P. J. DeMott, R. C. Sullivan, A. B. White, F. M. Ralph, P. Minnis, J. M. Comstock, J. M. Tomlinson and K. A. Prather, *Science*, 2013, **339**, 1572-1578.

16. N. M. Mahowald, A. R. Baker, G. Bergametti, N. Brooks, R. A. Duce, T. D. Jickells, N. Kubilay, J. M. Prospero and I. Tegen, *Glob. Biogeochem. Cycle*, 2005, **19**, GB4025, doi:4010.1029/2004GB002402.
17. C. R. Usher, A. E. Michel and V. H. Grassian, *Chem. Rev.*, 2003, **103**, 4883-4939.
18. J. N. Crowley, M. Ammann, R. A. Cox, R. G. Hynes, M. E. Jenkin, A. Mellouki, M. J. Rossi, J. Troe and T. J. Wallington, *Atmos. Chem. Phys.*, 2010, **10**, 9059-9223.
19. F. J. Dentener, G. R. Carmichael, Y. Zhang, J. Lelieveld and P. J. Crutzen, *J. Geophys. Res.-Atmos.*, 1996, **101**, 22869-22889.
20. T. D. Fairlie, D. J. Jacob, J. E. Dibb, B. Alexander, M. A. Avery, A. van Donkelaar and L. Zhang, *Atmos. Chem. Phys.*, 2010, **10**, 3999-4012.
21. A. Laskin, M. J. Iedema, A. Ichkovich, E. R. Graber, I. Taraniuk and Y. Rudich, *Faraday Discuss.*, 2005, **130**, 453-468.
22. A. Matsuki, Y. Iwasaka, G. Y. Shi, D. Z. Zhang, D. Trochkine, M. Yamada, Y. S. Kim, B. Chen, T. Nagatani, T. Miyazawa, M. Nagatani and H. Nakata, *Geophys. Res. Lett.*, 2005, **32**, L22806, doi: 22810.21029/22005gl024176.
23. R. C. Sullivan, S. A. Guazzotti, D. A. Sodeman and K. A. Prather, *Atmos. Chem. Phys.*, 2007, **7**, 1213-1236.
24. B. J. Krueger, V. H. Grassian, A. Laskin and J. P. Cowin, *Geophys. Res. Lett.*, 2003, **30**, 1148, doi: 1110.1029/2002gl016563.
25. K. D. Perry, S. S. Cliff and M. P. Jimenez-Cruz, *J. Geophys. Res.-Atmos*, 2004, **109**, D23S28, doi: 10.1029/2004JD004979.
26. E. R. Gibson, K. M. Gierlus, P. K. Hudson and V. H. Grassian, *Aerosol Sci. Technol.*, 2007, **41**, 914-924.
27. R. C. Sullivan, M. D. Petters, P. J. DeMott, S. M. Kreidenweis, H. Wex, D. Niedermeier, S. Hartmann, T. Clauss, F. Stratmann, P. Reitz, J. Schneider and B. Sierau, *Atmos. Chem. Phys.*, 2010, **10**, 11471-11487.
28. P. Reitz, C. Spindler, T. F. Mentel, L. Poulain, H. Wex, K. Mildenberger, D. Niedermeier, S. Hartmann, T. Clauss, F. Stratmann, R. C. Sullivan, P. J. DeMott, M. D. Petters, B. Sierau and J. Schneider, *Atmos. Chem. Phys.*, 2011, **11**, 7839-7858.
29. D. Niedermeier, S. Hartmann, T. Clauss, H. Wex, A. Kiselev, R. C. Sullivan, P. J. DeMott, M. D. Petters, P. Reitz, J. Schneider, E. Mikhailov, B. Sierau, O. Stetzer, B. Reimann, U. Bundke, R. A. Shaw, A. Buchholz, T. F. Mentel and F. Stratmann, *Atmos. Chem. Phys.*, 2011, **11**, 11131-11144.
30. Z. B. Shi, M. D. Krom, T. D. Jickells, S. Bonneville, K. S. Carslaw, N. Mihalopoulos, A. R. Baker and L. G. Benning, *Aeolian Res.*, 2012, **5**, 21-42.
31. S. Nickovic, A. Vukovic, M. Vujadinovic, V. Djurdjevic and G. Pejanovic, *Atmos. Chem. Phys.*, 2012, **12**, 845-855.
32. E. Journet, Y. Balkanski and S. P. Harrison, *Atmos. Chem. Phys.*, 2014, **14**, 3801-3816.
33. R. C. Sullivan, M. J. K. Moore, M. D. Petters, S. M. Kreidenweis, G. C. Roberts and K. A. Prather, *Atmos. Chem. Phys.*, 2009, **9**, 3303-3316.
34. D. F. Zhao, A. Buchholz, T. F. Mentel, K. P. Müller, J. Borchardt, A. Kiendler-Scharr, C. Spindler, R. Tillmann, A. Trimborn, T. Zhu and A. Wahner, *Atmos. Chem. Phys.*, 2010, **10**, 8601-8616.

35. R. A. Scanza, N. Mahowald, S. Ghan, C. S. Zender, J. F. Kok, X. Liu, Y. Zhang and S. Albani, *Atmos. Chem. Phys.*, 2015, **15**, 537-561.
36. J. T. Kelly, C. C. Chuang and A. S. Wexler, *Atmos. Environ.*, 2007, **41**, 2904-2916.
37. J. T. Kelly and A. S. Wexler, *J. Geophys. Res.-Atmos*, 2005, **110**, D11201, doi; 11210.11029/12004jd005583.
38. A. P. Prince, P. D. Kleiber, V. H. Grassian and M. A. Young, *Phys. Chem. Chem. Phys.*, 2008, **10**, 142-152.
39. Y. Liu, E. R. Gibson, J. P. Cain, H. Wang, V. H. Grassian and A. Laskin, *J. Phys. Chem. A*, 2008, **112**, 1561-1571.
40. A. Vlasenko, T. Huthwelker, H. W. Gaggeler and M. Ammann, *Phys. Chem. Chem. Phys.*, 2009, **11**, 7921-7930.
41. C. Wagner, G. Schuster and J. N. Crowley, *Atmos. Environ.*, 2009, **43**, 5001-5008.
42. M. J. Tang, J. Thieser, G. Schuster and J. N. Crowley, *Phys. Chem. Chem. Phys.*, 2012, **14**, 8551-8561.
43. Y. J. Liu, T. Zhu, D. F. Zhao and Z. F. Zhang, *Atmos. Chem. Phys.*, 2008, **8**, 7205-7215.
44. H. J. Li, T. Zhu, D. F. Zhao, Z. F. Zhang and Z. M. Chen, *Atmos. Chem. Phys.*, 2010, **10**, 463-474.
45. R. C. Sullivan, S. A. Guazzotti, D. A. Sodeman, Y. H. Tang, G. R. Carmichael and K. A. Prather, *Atmos. Environ.*, 2007, **41**, 7166-7179.
46. Y. Tobo, D. Zhang, A. Matsuki and Y. Iwasaka, *Proc. Natl. Acad. Sci. U. S. A.*, 2010, **107**, 17905-17910.
47. L. Li, Z. M. Chen, Y. H. Zhang, T. Zhu, J. L. Li and J. Ding, *Atmos. Chem. Phys.*, 2006, **6**, 2453-2464.
48. Q. Ma, H. He, Y. Liu, C. Liu and V. H. Grassian, *Phys. Chem. Chem. Phys.*, 2013, **15**, 19196-19204.
49. M. J. Tang, M. Q. Li and T. Zhu, *Sci. China-Chem.*, 2010, **53**, 2657-2662.
50. S. R. Tong, L. Y. Wu, M. F. Ge, W. G. Wang and Z. F. Pu, *Atmos. Chem. Phys.*, 2010, **10**, 7561-7574.
51. Q. X. Ma, Y. C. Liu, C. Liu and H. He, *Phys. Chem. Chem. Phys.*, 2012, **14**, 8403-8409.
52. A. H. Falkovich, G. Schkolnik, E. Ganor and Y. Rudich, *J. Geophys. Res.-Atmos.*, 2004, **109**, D02208, doi: 02210.01029/02003JD003919.
53. Y. Liu and A. Laskin, *J. Phys. Chem. A*, 2009, **113**, 1531-1538.
54. S. S. Brown, H. Stark, T. B. Ryerson, E. J. Williams, D. K. Nicks, M. Trainer, F. C. Fehsenfeld and A. R. Ravishankara, *J. Geophys. Res.-Atmos*, 2003, **108**, 4299.
55. J. N. Crowley, J. Thieser, M. J. Tang, G. Schuster, H. Bozem, Z. H. Beygi, H. Fischer, J. M. Diesch, F. Drewnick, S. Borrmann, W. Song, N. Yassaa, J. Williams, D. Pohler, U. Platt and J. Lelieveld, *Atmos. Chem. Phys.*, 2011, **11**, 10853-10870.
56. S. Seisel, C. Borensen, R. Vogt and R. Zellner, *Atmos. Chem. Phys.*, 2005, **5**, 3423-3432.
57. M. J. Tang, J. C. J. Camp, L. Rkiouak, J. McGregor, I. M. Watson, R. A. Cox, M. Kalberer, A. D. Ward and F. D. Pope, *J. Phys. Chem. A*, 2014, **118**, 8817-8827.

58. F. Karagulian, C. Santschi and M. J. Rossi, *Atmos. Chem. Phys.*, 2006, **6**, 1373-1388.
59. P. K. Mogili, P. D. Kleiber, M. A. Young and V. H. Grassian, *Atmos. Environ.*, 2006, **40**, 7401-7408.
60. C. Wagner, F. Hanisch, N. Holmes, H. de Coninck, G. Schuster and J. N. Crowley, *Atmos. Chem. Phys.*, 2008, **8**, 91-109.
61. M. J. Tang, G. Schuster and J. N. Crowley, *Atmos. Chem. Phys.*, 2014, **14**, 245-254.
62. G. C. Roberts and A. Nenes, *Aerosol Sci. Technol.*, 2005, **39**, 206-221.
63. N. Good, H. Coe and G. McFiggans, *Atmos. Meas. Tech.*, 2010, **3**, 1241-1254.
64. D. O. Topping, G. B. McFiggans and H. Coe, *Atmos. Chem. Phys.*, 2005, **5**, 1205-1222.
65. M. J. Tang, P. J. Telford, F. D. Pope, L. Rkiouak, N. L. Abraham, A. T. Archibald, P. Braesicke, J. A. Pyle, J. McGregor, I. M. Watson, R. A. Cox and M. Kalberer, *Atmos. Chem. Phys.*, 2014, **14**, 6035-6048.
66. M. J. Tang, R. A. Cox and M. Kalberer, *Atmos. Chem. Phys.*, 2014, **14**, 9233-9247.
67. M. D. Petters and S. M. Kreidenweis, *Atmos. Chem. Phys.*, 2007, **7**, 1961-1971.
68. P. Kumar, I. N. Sokolik and A. Nenes, *Atmos. Chem. Phys.*, 2011, **11**, 3527-3541.
69. P. Kumar, I. N. Sokolik and A. Nenes, *Atmos. Chem. Phys.*, 2011, **11**, 8661-8676.
70. S. Garimella, Y. W. Huang, J. S. Seewald and D. J. Cziczo, *Atmos. Chem. Phys.*, 2014, **14**, 6003-6019.
71. R. C. Sullivan, M. J. K. Moore, M. D. Petters, S. M. Kreidenweis, G. C. Roberts and K. A. Prather, *Phys. Chem. Chem. Phys.*, 2009, **11**, 7826-7837.
72. R. C. Sullivan, M. J. K. Moore, M. D. Petters, S. M. Kreidenweis, O. Qafoku, A. Laskin, G. C. Roberts and K. A. Prather, *Aerosol Sci. Technol.*, 2010, **44**, 830-846.
73. A. Vlasenko, S. Sjogren, E. Weingartner, K. Stemmler, H. W. Gaggeler and M. Ammann, *Atmos. Chem. Phys.*, 2006, **6**, 2147-2160.
74. M. D. Petters and S. M. Kreidenweis, *Atmos. Chem. Phys.*, 2008, **8**, 6273-6279.
75. M. J. Tang, J. Thieser, G. Schuster and J. N. Crowley, *Atmos. Chem. Phys.*, 2010, **10**, 2965-2974.
76. H. Herich, T. Tritscher, A. Wiacek, M. Gysel, E. Weingartner, U. Lohmann, U. Baltensperger and D. J. Cziczo, *Phys. Chem. Chem. Phys.*, 2009, **11**, 7804-7809.

Tables& Figures

Table 1. Dry mobility diameter (d_m), critical supersaturation (SSc) and CCN activity (κ) of calcium-containing salts.

Particle	d_m (nm)	SSc (%)	κ (this study)	κ (literature)
calcium nitrate, $Ca(NO_3)_2$	50	0.440	0.57	0.44-0.64 [33]
	50	0.432	0.59	
	70	0.262	0.59	
calcium chloride, $CaCl_2$	50	0.467	0.51	0.46-0.58 [33]
	50	0.464	0.52	
	70	0.273	0.54	
calcium sulfate, $CaSO_4$	200	0.222	0.034	0.0045±0.0012 [72]
	150	0.454	0.018	
	100	0.927	0.012	
calcium methanesulfonate, $Ca(CH_3SO_3)_2$	100	0.216	0.30	not measured previously
	70	0.327	0.38	
	70	0.326	0.38	
calcium formate, $Ca(HCOO)_2$	70	0.279	0.52	not measured previously
	50	0.460	0.47	
	50	0.460	0.47	
calcium acetate, $Ca(CH_3COO)_2$	70	0.294	0.47	not measured previously
	70	0.316	0.41	
	50	0.549	0.37	

Table 2. Critical supersaturation (SSc) and CCN activities (κ) of 200 nm fresh and aged $CaCO_3$ particles. Aged particles were generated by exposure of airborne $CaCO_3$ particles to N_2O_5 at 0% RH in an aerosol flow tube, with corresponding initial N_2O_5 concentrations, reaction time, and exposure also listed.

Particle	N_2O_5 (ppbv)	Time (s)	exposure (ppbv·s)	SSc (%)	κ
Fresh $CaCO_3$	--	--	--	0.703	0.0013
	--	--	--	0.567	0.0033
	--	--	--	0.609	0.0025
	--	--	--	0.653	0.0019
	--	--	--	0.597	0.0023
Aged $CaCO_3$	829	19.8	15041	0.233	0.0308
	349	19.8	6331	0.219	0.0351
	380	5.6	2142	0.231	0.0314
	97	5.6	547	0.295	0.0186
	110	14.1	1468	0.213	0.0370
	132	8.5	910	0.201	0.0418

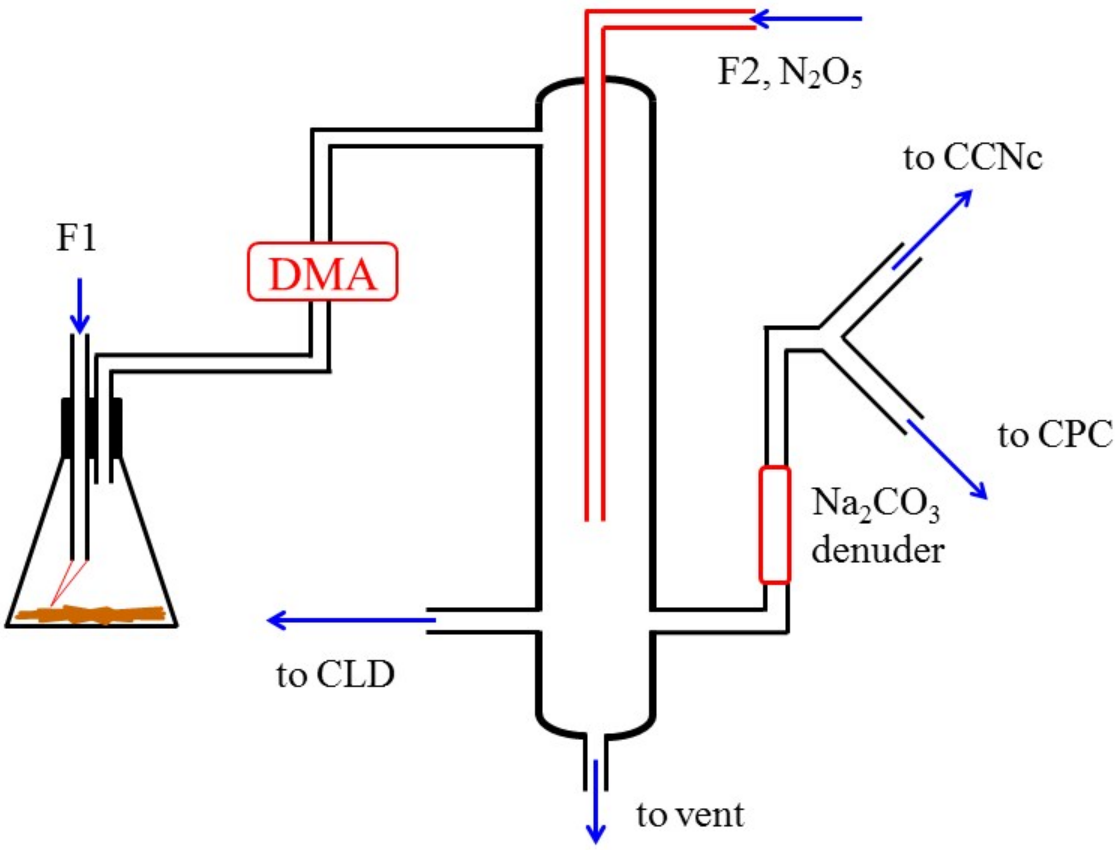

Figure 1. Schematic diagram of the experimental set-up used in this work. DMA: differential mobility analyser; CLD: chemiluminescence detector for nitrogen oxide quantification; CPC: condensation particle counter; CCNc: cloud condensation nuclei counter. F1 (1500 ml/min) was used to entrain dust particle into the air and F2 (5-10 ml/min) was used to introduce N_2O_5 into the flow tube.

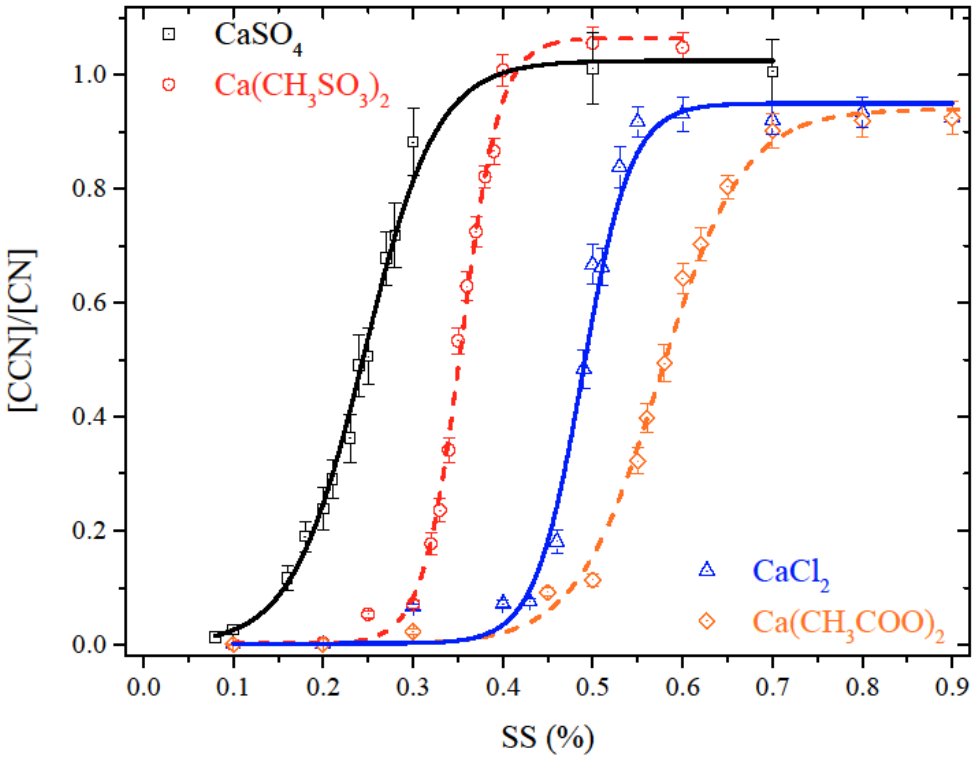

Figure 2. CCN activation curves of 200 nm $CaSO_4$ (black squares), 70 nm $Ca(CH_3SO_3)_2$ (red circles), 50 nm $CaCl_2$ (blue triangles), and 50 nm $Ca(CH_3COO)_2$ (orange diamonds). Please note that different particles diameters were used.

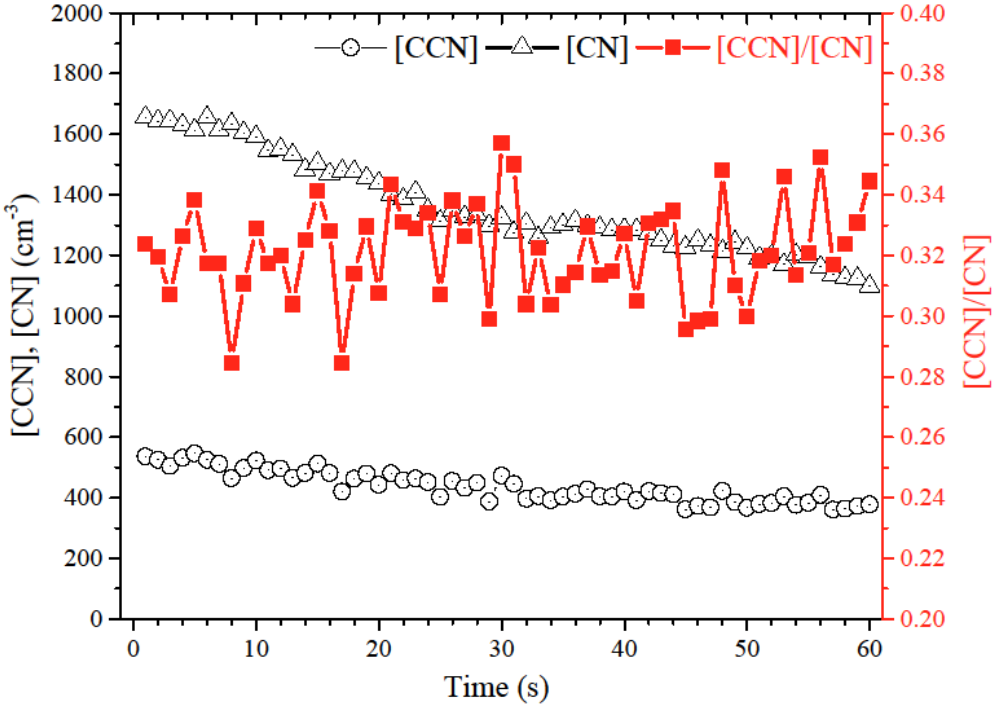

Figure 3. Typical dataset of measured number concentrations (left y-axis) of CCN (circles) and CN (triangles) for fresh $CaCO_3$ particles at a supersaturation of 0.50%. The activation fraction, [CCN]/[CN], is plotted on the right y-axis (squares).

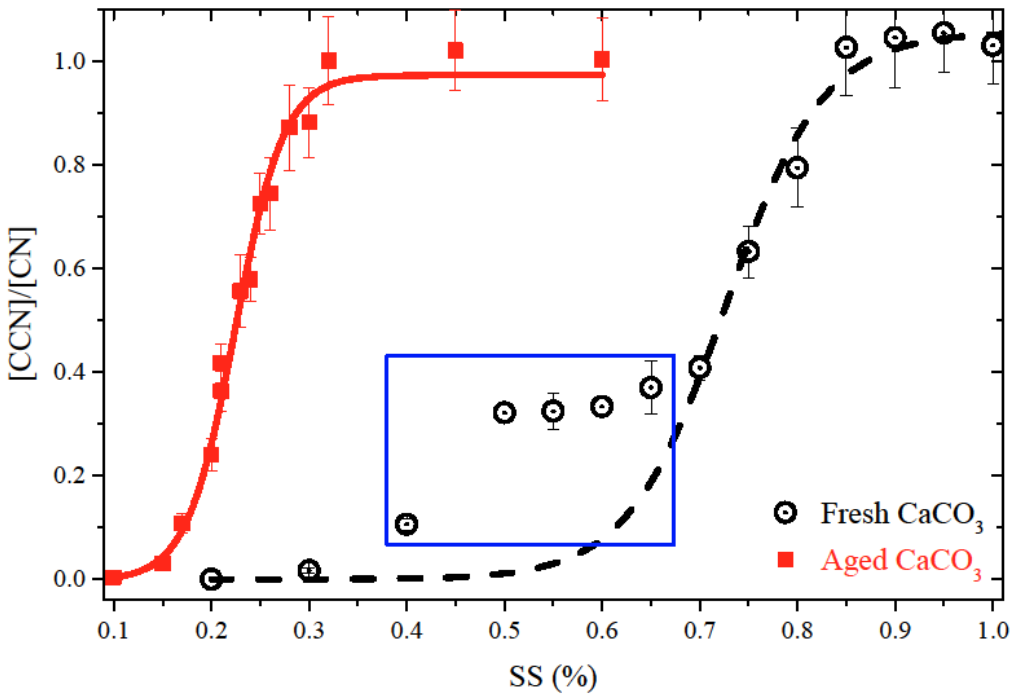

Figure 4. CCN activation curves of 200 nm fresh (circles) and aged (squares) $CaCO_3$ particles. The two curves are fitted activation curves for fresh and aged $CaCO_3$ particles. The plateau for fresh $CaCO_3$ particles is highlighted by the blue box, and details are provided in Section 3.3.

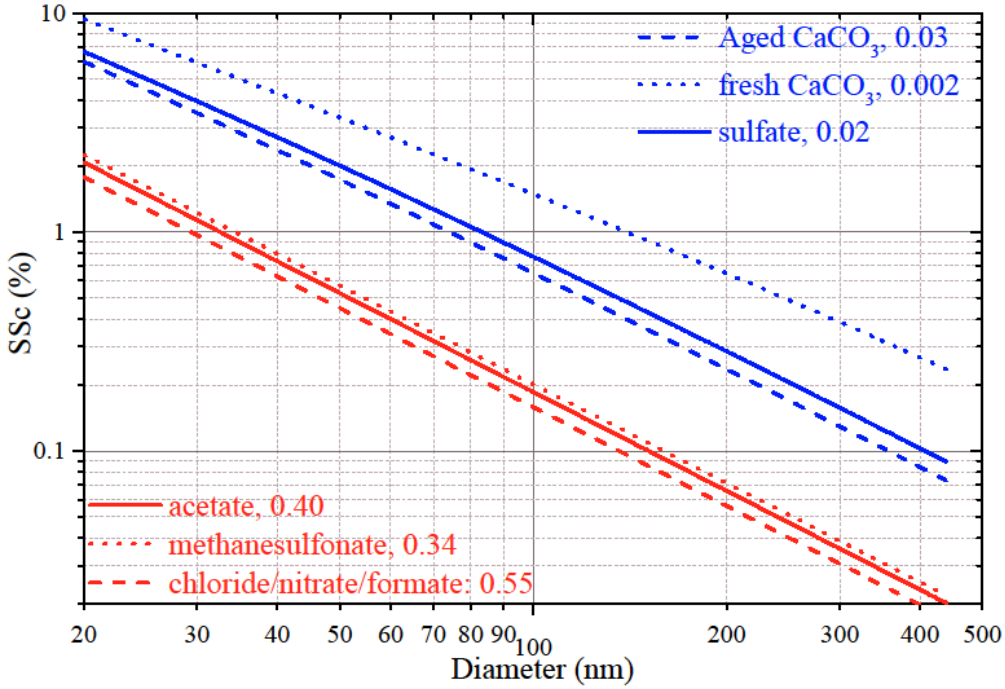

Figure 5. Critical supersaturation (%) as a function of diameter for pure Ca-containing compounds and aged $CaCO_3$ particles due to the reaction with N_2O_5 at 0% RH. This figure is produced using the average values of hygroscopicity parameters for each compounds determined in this study. The uncertainties (1 σ) in κ are estimated to be ±0.001 for fresh $CaCO_3$, ±0.01 for aged $CaCO_3$ and calcium sulfate, ±0.05 for other Ca-containing compounds, based on the measurements summarized in Tables 1-2.

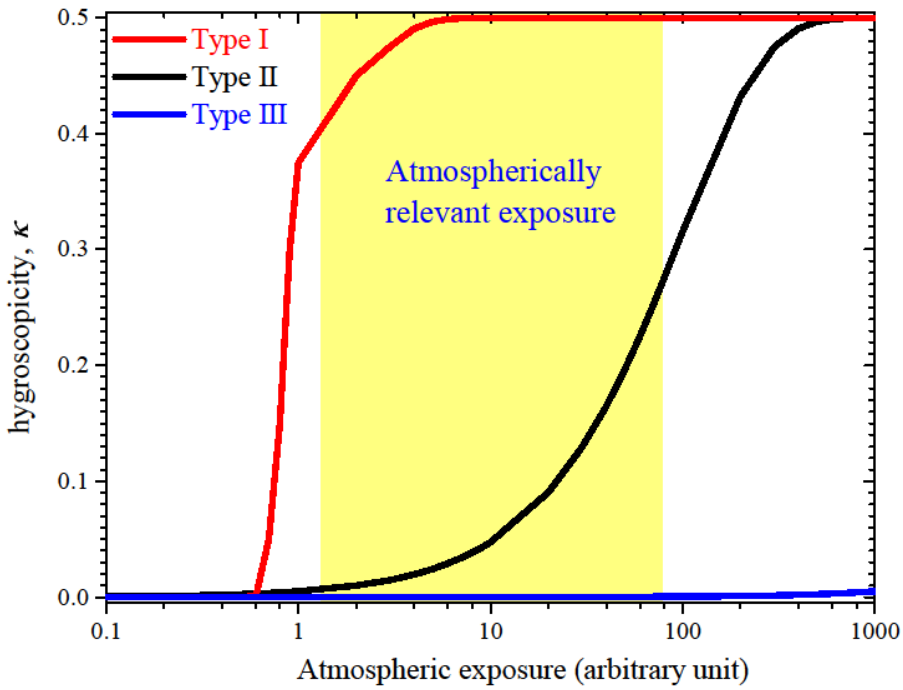

Figure 6. Schematic diagram of three theoretical kinetics regimes of hygroscopicity change of mineral dust particles due to atmospheric heterogeneous reactions, illustrating the importance of the kinetics of chemical reactions affecting κ in the ambient atmosphere.